

# Parietal-Frontal Pathway Controls Relapse of Fear Memory in a Novel Context

Bitna Joo, Shijie Xu, Hyungju Park, Kipom Kim, Jong-Cheol Rah, and Ja Wook Koo

## ABSTRACT

**BACKGROUND:** Fear responses significantly affect daily life and shape our approach to uncertainty. However, the potential resurgence of fear in unfamiliar situations poses a significant challenge to exposure-based therapies for maladaptive fear responses. Nonetheless, how novel contextual stimuli are associated with the relapse of extinguished fear remains unknown.

**METHODS:** Using a context-dependent fear renewal model, the functional circuits and underlying mechanisms of the posterior parietal cortex (PPC) and anterior cingulate cortex (ACC) were investigated using optogenetic, histological, in vivo, and ex vivo electrophysiological and pharmacological techniques.

**RESULTS:** We demonstrated that the PPC-to-ACC pathway governs fear relapse in a novel context. We observed enhanced populational calcium activity in the ACC neurons that received projections from the PPC and increased synaptic activity in the basolateral amygdala-projecting PPC-to-ACC neurons upon renewal in a novel context, where excitatory postsynaptic currents amplitudes increased but inhibitory postsynaptic current amplitudes decreased. In addition, we found that parvalbumin-expressing interneurons controlled novel context-dependent fear renewal, which was blocked by the chronic administration of fluoxetine.

**CONCLUSIONS:** Our findings highlight the PPC-to-ACC pathway in mediating the relapse of extinguished fear in novel contexts, thereby contributing significant insights into the intricate neural mechanisms that govern fear renewal.

<https://doi.org/10.1016/j.bpsgos.2024.100315>

Appropriate behavioral responses to environmental threat signals are important for animal survival. Disrupted fear regulation can contribute to disorders such as posttraumatic stress disorder, anxiety disorder, and other fear-related disorders that are often characterized by an exaggerated fear response to innocuous situations or stimuli (1,2). Although strides have been made in applying extinction learning to ameliorate these disorders, it is essential to recognize that certain conditions may precipitate relapse (3).

Auditory fear conditioning is a valuable paradigm for investigating the intricacies of fear memory formation. Moreover, the enduring imprint left by pairing a tone (conditioned stimulus [CS]) with an aversive foot shock (unconditioned stimulus [US]) underscores the lasting impact of associative learning (4–6). Importantly, the context independence of the initial CS-US associations during retrieval (7,8) contrasts sharply with the context-dependent nature of extinguishing this fear memory (5,9). Therefore, fear extinction transpires exclusively within the specific extinction training context, and extinguished fear exhibits a proclivity to rapidly resurface when subjected to a different context, a phenomenon recognized as fear renewal (3,5,9). ABC renewal describes the renewal of a previously extinguished conditioned response when the CS is presented in a context different from the initial pairing or extinction. It remains unknown how novel contextual stimuli are associated with the relapse of extinguished fears.

Several studies have reported that cortical networks play a critical role in predicting outcomes in response to contextual changes (7,10,11). Cortical networks integrate multimodal sensory information as well as motor-related information to drive adequate behavior in response to a given situation (12,13). Particularly, the posterior parietal cortex (PPC), a key association area reciprocally connected to several sensory areas including the somatosensory, visual, and auditory cortices, is involved in certain cognitive behaviors, including attention, intention, and decision making (14–24). Recent studies have demonstrated that the PPC plays an important role in memory updating in an experience-dependent manner (25) and in prediction updating with new sensory inputs (26), possibly by integrating new information with ongoing activity dynamics, as in evidence-accumulation tasks (27,28). Thus, it is conceivable that the PPC regulates the relapse of extinguished fear memories in a novel context (29). However, the neural circuits and mechanisms that underlie the regulation of novel context-dependent fear relapse by PPC remain unexplored.

The anterior cingulate cortex (ACC), which has reciprocal projections to the PPC, has been extensively studied for the regulation of fear behaviors, particularly in the storage of contextual fear memory (9,14,30). A lesion study has shown that inactivation of the ACC disrupts the retrieval of remote contextual fear memories (31). The ACC inputs to the

basolateral amygdala (BLA) to regulate innate and observational fear responses (32–34). However, the circuit- and cell type-specific mechanisms in the ACC underlying the abnormal information processing that produces an excessive fear response in new contexts are not well understood.

## METHODS AND MATERIALS

### Animals

All experimental procedures were conducted in accordance with the guidelines established by the Institutional Animal Care and Use Committee of the Korea Brain Research Institute (IACUC-22-00028). Animals were maintained under a 12-hour light/dark cycle (lights on at 08:00 AM) and had ad libitum access to food and water. We used 5- to 10-week-old C57BL/6N wild-type (Orient), PV-Cre (Pvalb<sup>tm1(cre)Arbr/J</sup>, The Jackson Laboratory), and Ai9 (Gt(ROSA)26Sor<sup>tm9(CAG-tdTomato)Hze/J</sup>, The Jackson Laboratory) mice. The mice were randomly assigned to each group.

### Stereotaxic Surgeries

All surgeries were conducted under anesthesia administered intraperitoneally, comprising a mixture of ketamine (100 mg/kg) and xylazine (10 mg/kg) in 0.1-M phosphate-buffered saline. A Hamilton syringe with a 33-gauge needle (Hamilton) was used for all viral injections. The virus was injected bilaterally at a rate of 0.1  $\mu$ L/min, and a total of 0.5  $\mu$ L was administered to each hemisphere. After injection, the needle was left in place for at least 10 minutes to allow the diffusion of the virus at the injection site.

### Fear Behavioral Assays

The mice were conditioned using a fear conditioning system (Panlab Harvard Apparatus). The test was performed using a methacrylate apparatus (250  $\times$  250  $\times$  250 mm) located inside a sound-attenuating box (670  $\times$  530  $\times$  550 mm). For fear conditioning (context A), a black methacrylate wall and an electric floor grid were used. The extinction context (context B) consisted of a white wall and metallic plate, and the novel renewal context (context C) consisted of black- and yellow-striped paper walls and floors.

### Statistical Analysis

Data analysis was performed using customized scripts in MATLAB (2021a; The MathWorks, Inc.) and LabVIEW (National Instruments). Statistical analyses were conducted using Prism software. Parametric and nonparametric tests were used as appropriate, and normality was assessed using the D'Agostino-Pearson and Kolmogorov-Smirnov tests to verify the suitability of the following statistical analyses. The statistical tests used in this study included the *t* test, Mann-Whitney *U* test, 1-way analysis of variance (ANOVA), 2-way ANOVA, and 2-way repeated-measures (RM) ANOVA. All data are presented as mean  $\pm$  SEM.

## RESULTS

### Parietal-Frontal Circuit Regulates Fear Renewal in a Novel Context

To understand how contextual factors influence the role of the PPC in fear memory relapse, the 2 fear renewal models

are employed: ABA versus ABC renewal. After the extinction phase, the association between an auditory cue (CS) and an aversive shock (US) is weakened; however, fear memory is not entirely erased (5,7,9). In contrast to highly context-dependent fear extinction (4,6,9), fear memory relapse can occur when the CS is presented outside the extinction context, irrespective of whether this is the conditioning context (ABA renewal) or a novel context to which mice have never been exposed before (ABC renewal) (9,12,35). First, we examined the validation of fear renewal across different contexts (context A and C) following fear conditioning (context A) and extinction sessions (context B) (Figure S1A). The results revealed distinct patterns of fear response in these contexts (Figure S1B, C).

Our previous study demonstrated that the PPC plays a role in ABC, but not ABA, renewal (29). Nevertheless, there is currently no evidence to support the involvement of the PPC circuitry in ABC renewal. The PPC predominantly projects to the ACC, but the ACC showed a relatively rare projection to the PPC (14). The only suggestive information comes from a prior observation that PPC projections to the ACC, a medial prefrontal cortex subregion associated with contextual fear memory (31,36,37), have been linked to experience-dependent fear memory updating (25). To investigate the contribution of the PPC  $\rightarrow$  ACC circuitry in the renewal of conditioned fear in a novel context after extinction, i.e., ABC renewal (Figure 1A), we used an optogenetic silencing approach by expressing AAVs (adeno-associated viruses) carrying halorhodopsin fused with enhanced yellow fluorescent protein (NpHR) or enhanced YFP (yellow fluorescent protein) in the bilateral PPC and implanted optic fibers into the ACC (Figure 1A–C). Mice injected with NpHR or YFP were exposed to a novel context under multiple ON-OFF optogenetic inhibitions, followed by fear conditioning and extinction (Figure 1D). We observed significantly attenuated freezing in NpHR mice compared with YFP-expressing mice during the light-on trial (Figure 1D, E). Notably, there was no significant difference in freezing behavior between the YFP and NpHR groups before the renewal sessions (group effect,  $F_{1,13} = 0.2072$ ,  $p = .6565$ ; time effect,  $F_{3,633,47.23} = 21.74$ ,  $p < .0001$ ; group  $\times$  time interaction,  $F_{18,234} = 0.7911$ ,  $p = .7100$ ; 2-way RM ANOVA). Optogenetic inhibition of the PPC  $\rightarrow$  ACC circuit had a selective effect on the first CS presentation (ON session) but did not significantly alter subsequent responses (group effect,  $F_{1,13} = 8.090$ ,  $p = .0138$ ; time effect,  $F_{2,594,33.73} = 8.193$ ,  $p = .0005$ ; group  $\times$  time interaction,  $F_{4,52} = 2.465$ ,  $p = .0564$ ; YFP-Sound 1 ON vs. NpHR-Sound 1 ON:  $p = .00138$ ; YFP-Sound 2 OFF vs. NpHR-Sound 2 OFF:  $p = .4111$ ; YFP-Sound 3 ON vs. NpHR-Sound 3 ON:  $p = .9437$ ; YFP-Sound 4 OFF vs. NpHR-Sound 4 OFF:  $p = .1761$ ; YFP-Sound 5 ON vs. NpHR-Sound 5 ON:  $p = .9779$ ; 2-way RM ANOVA with Sidák's multiple comparisons tests). This observation implies that the PPC  $\rightarrow$  ACC circuit is primarily concentrated in the initial stages of fear renewal rather than being continuously maintained throughout multiple CS presentations. The temporal specificity of this effect highlights the importance of a new environment for PPC action. To evaluate the sufficiency of PPC  $\rightarrow$  ACC activity for ABC renewal, we expressed AAV vectors encoding excitatory ChR2 (channelrhodopsin-2) or YFP in the PPC and implanted an optic fiber in the ACC (Figure 1F). Activation of the PPC-ACC circuit was

Parietal-Frontal Pathway Controls ABC Renewal

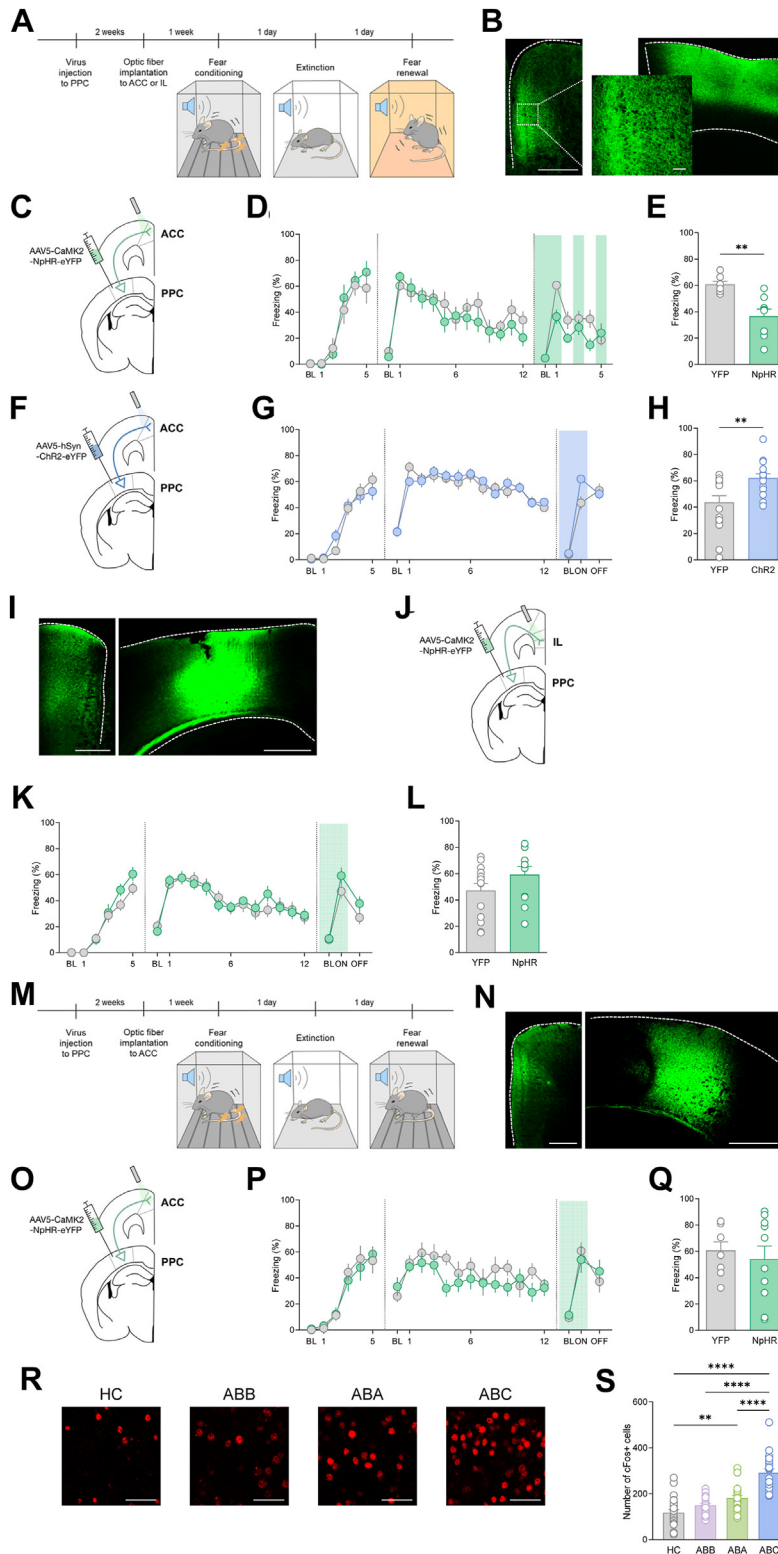


**Figure 1.** Optogenetic manipulation of the PPC-to-prefrontal cortex circuits in fear renewal. **(A)** Schematic representation of the experimental schedule for the optogenetic manipulation of the PPC→prefrontal cortex terminals during ABC renewal. **(B)** Representative images show the injection site of AAV5-CaMK2-NpHR-eYFP in the PPC (right) and YFP immunofluorescence in the ACC (left). Enlarged image showing the axon terminal expression of YFP in the ACC. Scale bars = 500 μm and 50 μm (insets). **(C)** Schematic of the experimental design for viral infection and optic fiber implantation for optogenetic inhibition of the PPC→ACC circuit. **(D)** ABC renewal with optogenetic inactivation of PPC→ACC projections (group effect,  $F_{1,13} = 0.8410$ ,  $p = .3758$ ; time effect,  $F_{24,312} = 21.34$ ,  $****p < .0001$ ; group × time interaction,  $F_{24,312} = 1.201$ ,  $p = .2382$ ; 2-way RM ANOVA). **(E)** The NpHR group showed significantly reduced fear responses during optogenetic inhibition ( $**p = .0022$ , 2-tailed unpaired  $t$  test;  $N = 7$  and 8 for YFP and NpHR, respectively). **(F)** Schematic of the experimental design for the photoactivation of the PPC→ACC circuit with AAV5-hSyn-ChR2-eYFP. **(G)** ABC renewal with optogenetic activation of the PPC→ACC circuit (group effect,  $F_{1,29} = 0.1543$ ,  $p = .6973$ ; time effect,  $F_{21,609} = 69.70$ ,  $****p < .0001$ ; group × time interaction,  $F_{21,609} = 1.437$ ,  $p = .0939$ ; 2-way RM ANOVA). **(H)** Optogenetic activation of PPC→ACC projections significantly enhanced freezing during ABC renewal ( $**p = .0054$ , 2-tailed unpaired  $t$  test;  $N = 16$  and 15 for YFP and ChR2, respectively). **(I)** Representative images show the injection site of AAV5-CaMK2-NpHR-eYFP in the PPC (right) and eYFP immunofluorescence in the IL (left). Scale bar = 500 μm. **(J)** Schematic of the experimental design for the photoinhibition of PPC→IL projections with AAV5-CaMK2-NpHR-eYFP. **(K)** ABC renewal with optogenetic inhibition of PPC→IL projections (group effect,  $F_{1,23} = 0.3999$ ,  $p = .5334$ ; time effect,  $F_{21,483} = 34.13$ ,  $****p < .0001$ ; group × time interaction,  $F_{21,483} = 0.8786$ ,  $p = 0.6197$ ; 2-way RM ANOVA). **(L)** Photoinhibition of the PPC→IL circuit did not affect the fear response ( $p = .1558$ , 2-tailed unpaired  $t$  test;  $n = 14$  and 11 for YFP and NpHR, respectively). **(M)** Schematic of the experimental schedule for ABA renewal. **(N)** Representative images show the injection site of AAV5-CaMK2-NpHR-eYFP in the PPC (right) and eYFP immunofluorescence in the ACC (left). Scale bar = 500 μm. **(O)** Schematic of the viral strategy for inactivation of PPC→ACC projections. **(P)** ABA renewal with optogenetic inhibition of the PPC→ACC circuit (group effect,  $F_{1,16} = 0.4714$ ,  $p = .5022$ ; time effect,  $F_{21,336} = 17.54$ ,  $****p < .0001$ ; group × time interaction,  $F_{21,336} = 1.028$ ,  $p = .4282$ ; 2-way RM ANOVA). **(Q)** Photoinhibition of the PPC→ACC projections did not change the fear response ( $p = .6018$ , 2-tailed unpaired  $t$  test;  $N = 8$  and 10 for YFP and NpHR, respectively). **(R)** Confocal images from representative brain slices of the PPC showing cFos+ cells in the experimental group (HC; extinction retrieval, ABB; ABA renewal; ABC renewal). **(S)** Quantification of cFos+ cells after behavioral sessions ( $F_{3,89} = 34.10$ ,  $****p < .0001$ ; HC vs. ABA:  $**p = .0023$ ; HC vs. ABC:  $****p < .0001$ ; ABB vs. ABC:  $****p < .0001$ ; ABA vs. ABC:  $****p < .0001$ , 1-way ANOVA with Tukey's multiple comparison

test;  $n = 24$  slices/8 mice for HC, ABB, and ABA, and  $n = 21$  slices/7 mice for ABC). ACC, anterior cingulate cortex; BL, baseline; HC, home cage; IL, infralimbic cortex; PPC, posterior parietal cortex; RM ANOVA, repeated measures analysis of variance; YFP, yellow fluorescent protein.

sufficient to evoke an enhanced fear response in the Chr2 group compared with that in YFP-expressing mice (Figure 1G, H).

We wondered whether ventral hippocampal (vHPC) projections to the infralimbic cortex (IL) circuit (vHPC→IL) also mediate ABC renewal because prior research has shown that this circuit is significant for fear renewal in the conditioning context, i.e., ABA renewal (38). Photoinhibition of the IL pathway by vHPC during ABC renewal did not alter the fear response (Figure S1A–E). In addition, no significant differences were observed when PPC→IL terminal was inhibited (Figure 1I–L). Inactivation of the PPC→ACC pathway did not alter ABA renewal (Figure 1M–Q). These data are consistent with our previous report that PPC regulates ABC renewal but not ABA renewal or reinstatement or fear retrieval (29). In addition, photoinhibition of the PPC during fear conditioning and extinction did not alter ABC renewal (Figure S1F–K). Activation of the PPC did not change fear expression in the extinction context (extinction retrieval; ABB), which implies that increasing the activity of the PPC does not evoke fear relapse (Figure S1L–O). Overall, it is suggested that there are parallel pathways between these 2 renewal models: the PPC→ACC circuit for ABC renewal and the vHPC→IL circuit for ABA renewal.

Next, we quantified the activated cells by immunostaining after exposing mice to different contextual conditions, including home cage (HC), ABB, ABA, and ABC. The number of c-Fos+ cells was significantly higher in the ABC group than in the HC, ABB, and ABA groups (Figure 1R, S). These findings are consistent with the idea that the PPC reflects different contextual situations.

Next, we investigated the physiological properties of ACC-projecting PPC neurons under different behavioral conditions (Figure S3). Analyses of spontaneous excitatory postsynaptic currents (EPSCs) and spontaneous inhibitory postsynaptic currents (IPSCs), intrinsic properties, and neuronal excitability revealed no significant changes across different behavioral conditions (Figure S3B–S). Taken together, these results suggest that the ACC is the functional output region of the PPC and that the PPC→ACC pathway is specifically responsible for the relapse of fear memory in a novel context.

### In Vivo Ca<sup>2+</sup> Recording During ABC Renewal Reveals Changes in PPC→ACC Dynamics

To determine whether the ACC neural activity receiving inputs from the PPC is precisely locked on the fear response in a novel “C” context, we injected AAVs carrying trans-synaptic Cre recombinase (Cre) into the PPC and a genetically encoded fluorescent Ca<sup>2+</sup> indicator (GCaMP) into the ACC, and placed optical fibers over the ACC (Figure 2A–C) (39,40). During fear conditioning, early extinction, late extinction, and extinction retrieval, Ca<sup>2+</sup> activity did not differ before and after the presentation of CSs (Figure 2D–I, 2N–O). However, PPC→ACC neurons showed significant responses to CSs during fear renewal in the novel context (Figure 2J–L). In addition, event frequency was enhanced during renewal (Figure 2M). Interestingly, the Ca<sup>2+</sup> signal was activated only when the integration of tone CS with a novel context occurred, whereas the activity was not responsive to context C without

tone CS, emphasizing the importance of PPC→ACC neurons in the integration of multisensory signals. Collectively, these results support a functional requirement for the PPC→ACC connection in ABC fear renewal, indicating differential dynamics according to the fear state.

### Fear States Do Not Alter the PPC→ACC Projection Profile

We investigated whether fear renewal produces permanent structural changes in ACC neurons that receive inputs from the PPC. The combined use of a transgenic mouse line carrying floxed-stop-tdTomato (Ai9) and AAV-mediated trans-synaptic Cre expression allowed the visualization of postsynaptic ACC neurons that received inputs from the PPC (Figure 3A, B). Furthermore, excitatory (CaMKII [calcium/calmodulin-stimulated protein kinase II] [green]) and inhibitory (parvalbumin [PV] [magenta]) neuron markers were costained with PPC→ACC neurons (tdTomato+ [tdT+] [red]). tdT+ PPC→ACC cells were observed in layers 1, 2/3, and 5 and were mainly distributed in layers 2/3 and 5. No significant changes in the number of PPC→ACC neurons were observed (Figure 3C). The number of double-positive neurons did not differ significantly (Figure 3D, E). However, CaMKII+ postsynaptic ACC cells showed more connections to the PPC than to the PV+ cells in all groups (Figure 3F). Taken together, these structural characterizations suggest that the fear state does not affect the number of PPC projection targets in the ACC.

### PPC-Driven Synaptic Activity in BLA-Projecting ACC Neurons Is Increased in ABC Renewal

Next, we examined the role of ACC projections to the BLA, a key brain region in the regulation of fear responses to threats, during ABC renewal (41–43). We injected retrograde inhibitory opsin Jaws into the BLA to transiently silence monosynaptic ACC projections to the BLA (Figure 4A, B) (33). Consistent with our PPC→ACC manipulation results, photoinhibition of ACC neurons innervating the BLA significantly blocked the return of fear in the novel context (Figure 4C, D). These results emphasize the importance of the parietal-frontal pathway, upstream of the BLA, in ABC renewal.

Based on these results, we wondered about the nature of PPC→ACC→BLA synaptic transmission. We recorded ACC neurons innervating the BLA after fear behaviors. ACC neurons that expressed mCherry and projected to the BLA without the concurrent expression of Chr2 were recorded under optogenetic excitation (Figure 4E). Photostimulation increased the excitation/inhibition ratio in the ABC group compared with that in the HC, ABB, and ABA groups. To determine that the light-evoked responses are glutamatergic and GABAergic (gamma-aminobutyric acid), we sequentially administered AP5, NBQX, and bicuculline. EPSCs were abolished by treatment with AP5 and NBQX, and IPSCs were completely diminished by further application of bicuculline (Figure 4F). Photostimulation of ACC neurons receiving inputs from the PPC modulated synaptic transmission in ACC neurons projecting to the BLA by increasing the EPSC amplitude and decreasing the IPSC amplitude (Figure 4F–I). There were no significant group differences in onset latency (Figure 4J).

Parietal-Frontal Pathway Controls ABC Renewal

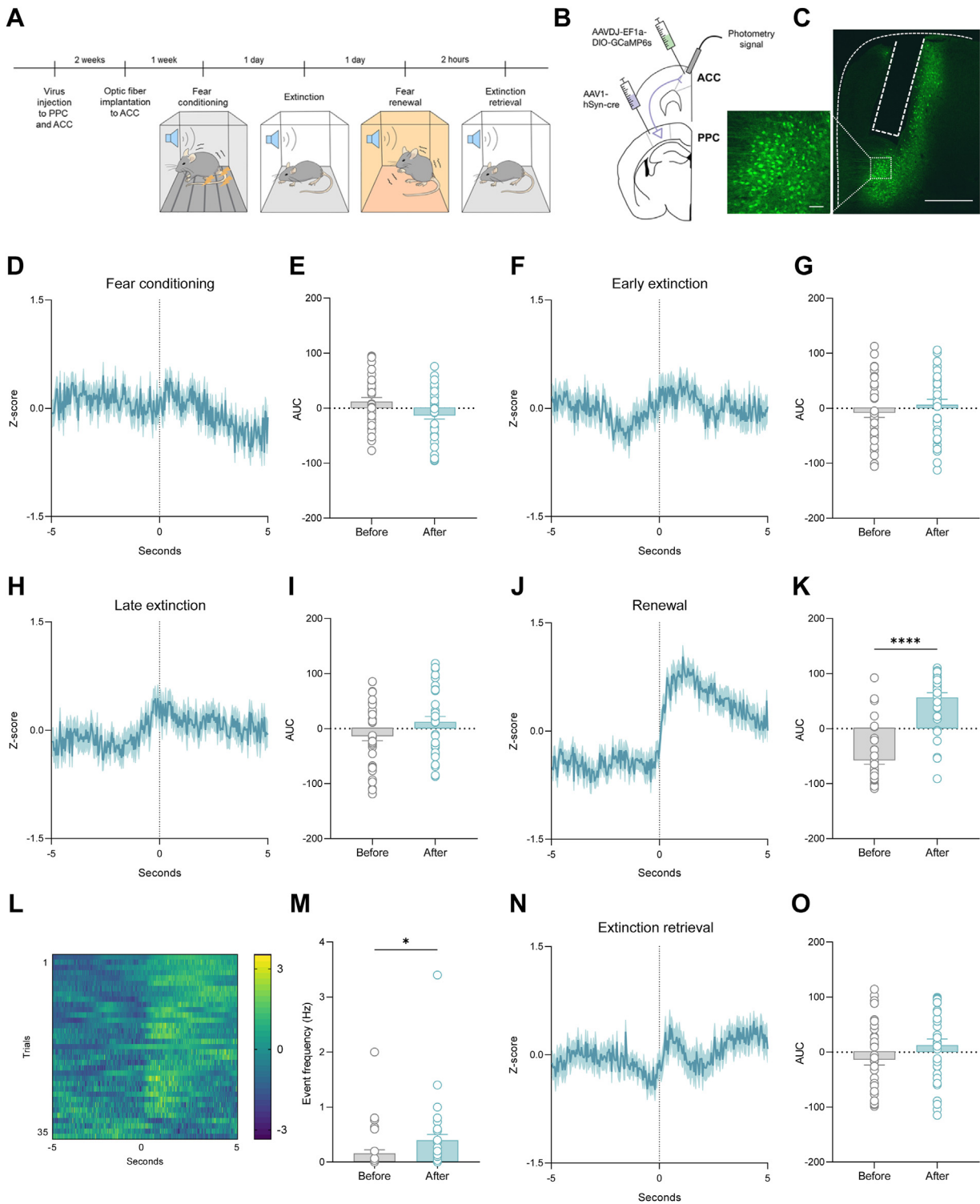


**Figure 2.** Populational calcium dynamics of ACC neurons that receive projections from PPC during fear conditioning, extinction, renewal, and extinction retrieval. **(A)** Schematic representation of the behavioral schedule for the fiber photometry recordings. **(B)** Experimental design for PPC→ACC projection-specific calcium imaging in the ACC. Cre-dependent GCaMP6s are selectively expressed in the ACC, which receives projections from the PPC. **(C)** Representative image showing GCaMP6s-expressing PPC→ACC neurons with the tip of an optic fiber placement. Scale bars = 500  $\mu$ m and 50  $\mu$ m (insets). **(D)** Average z-scored PPC→ACC GCaMP6s activity on fear conditioning. **(E)** Boxplots of the AUC before and after presentation of the CS during fear conditioning ( $p = .1189$ , 2-tailed paired  $t$  test;  $n = 35$  trials/7 mice). **(F)** Average z-scored PPC→ACC GCaMP6s activity during early extinction. **(G)** Boxplots of the AUC

Next, we recorded spontaneous release events. The amplitude of the spontaneous EPSCs did not differ among groups (Figure 4K–M). However, there was an increase in the frequency of spontaneous EPSCs and a significant shift toward a faster frequency in the ABC group, although statistical significance for the average frequency was found only between the HC and ABC groups (Figure 4P, Q). In contrast, no changes were detected in the amplitude or frequency of spontaneous IPSCs (Figure 4K, N, O, R, S). Additionally, there were no differences in the intrinsic properties and excitability (Figure S4). Collectively, these results demonstrate that the local synaptic activity of the PPC-input-receiving ACC neurons that project to the BLA is significantly increased only during ABC renewal.

### PPC-to-ACC<sup>PV</sup> Neurons Switch Fear State in a Novel Context

Because PPC→ACC activation alters network excitability in the ACC circuits, we reasoned that manipulation of the local cell population may control the fear response during ABC renewal. PV neurons are a major interneuron population that primarily target the soma of pyramidal neurons, and their circuit mechanisms have been identified (44–46). Moreover, as a subset of ACC neurons expressing PV (Figure 3), we sought to determine whether they also contribute to the ABC renewal behavior.

To test this hypothesis, we used a viral-genetic intersectional expression strategy to specifically target PV+ ACC interneurons that receive PPC inputs (PPC→ACC<sup>PV</sup>). Trans-synaptic Flp was injected into the PPC, and Cre- and Flp-codendent constructs (ConFon-NpHR or ConFon-ChR2) were injected and optical fibers were implanted into the ACC of PV-Cre mice (Figure 5A–C, F). The inhibition of PPC→ACC<sup>PV</sup> neurons robustly induced a fear response in a novel context (Figure 5D, E). Conversely, activation of the PPC→ACC<sup>PV</sup> pathway attenuated the relapse of extinguished CS (Figure 5G–H). Intriguingly, these effects were not detected when PV neurons were activated in the ACC (Figure S5), suggesting that the subpopulation of PV neurons receiving input from the PPC is important. These results demonstrate that PPC→ACC<sup>PV</sup> interneurons are necessary and sufficient for switching fear states during the relapse of fear memory in a novel context.

Furthermore, it is questionable whether manipulation of non-PV neurons using cell type- and circuit-specific optogenetics (CoffFon-NpHR) would yield distinct results, primarily affecting excitatory populations. Unlike the inhibition of PV neurons (ConFon-NpHR), the CoffFon-NpHR group showed a decreased fear response in the novel context (Figure 5I–L). Additionally, when these excitatory populations were activated (CoffFon-ChR2), the fear response increased, demonstrating a reverse behavior compared to the photostimulating PV

inhibitory populations (Figure 5M–O). Furthermore, during the light-off session, a significant difference in freezing behavior was observed between the mCherry and ConFon-ChR2 groups ( $p = .0050$ , 2-tailed unpaired  $t$  test,  $N = 16$  and  $18$  for YFP and ChR2, respectively). However, no difference was observed between the mCherry and CoffFon-ChR2 groups ( $p = .063$ , 2-tailed unpaired  $t$  test,  $N = 9$  and  $8$  for mCherry and ChR2, respectively). While we cannot completely exclude the possibility of retrograde labeling effects, histological analysis demonstrates red fluorescence in ACC neuron somas following viral tracing from the PPC (Figure S6). Consistent with previous intersectional methods, this finding underscores the consistency of our results and confirms the specificity of labeling ACC neurons without detecting fluorescence in the PPC (39,47,48).

This result suggests that direct activation of PV neurons in the ACC does not influence the reactivation of fear memory during ABC renewal. Instead, it highlights the importance of a specific subpopulation of PV neurons that receives input from the PPC. These findings not only emphasize the interplay within neural circuits but also highlight specific neuronal populations, particularly within PV neurons, that can be targeted to modulate fear responses, with potential implications for fear-related disorders.

### Selective Serotonin Reuptake Inhibitor Treatment Attenuates Circuit- and Cell Type-Specific Induction of Fear Relapse

Having established that PPC→ACC<sup>PV</sup> interneurons regulate ABC renewal, we next investigated how the clinical drug fluoxetine (Flx), a broad-spectrum medication used for the treatment of various fear-related psychiatric disorders (49–52), influences the PPC→ACC pathway in ABC renewal. Several studies have shown that chronic fluoxetine treatment facilitates extinction and reduces freezing during extinction retrieval and ABA renewal (50–52). Moreover, chronic fluoxetine administration attenuated the PV deficit induced by the combined stress; however, this effect was not observed at the somatostatin level (53). However, the effects of fluoxetine on ABC renewal and related circuits have yet to be explored.

To determine whether fluoxetine can influence ABC renewal induced by the photoinactivation of PPC→ACC<sup>PV</sup> interneurons, we infused ConFon-NpHR into PV-Cre mice, and fluoxetine or saline (Sal) was administered chronically between the periods of extinction and renewal (Figure 6A–C). Fluoxetine injections effectively diminished the relapse of the extinguished fear response (YFP+Sal – YFP+Flx) (Figure 6D, E). Consistent with the above results, the NpHR+Sal group showed a higher level of fear response than the YFP+Sal group. Importantly, fluoxetine injections effectively blocked the optogenetically induced high levels of fear response

before and after the presentation of CS during early extinction ( $p = .5023$ , 2-tailed paired  $t$  test;  $n = 35$  trials/7 mice). (H) Average z-scored PPC→ACC GCaMP6s activity on late extinction. (I) Boxplots of the AUC before and after the presentation of CS during late extinction ( $p = .2250$ , 2-tailed paired  $t$  test;  $n = 35$  trials/7 mice). (J) Average z-scored PPC→ACC GCaMP6s activity in ABC renewal. (K) Boxplots of the AUC before and after presentation of CS during ABC renewal (\*\*\*\* $p < .0001$ , 2-tailed paired  $t$  test;  $n = 35$  trials/7 mice). (L) Heatmap of ACC fluorescence aligned with the onset of CS during ABC renewal. (M) Event frequency was enhanced during ABC renewal (\* $p = .021$ , 1-tailed paired  $t$  test). (N) Average z-scored PPC→ACC GCaMP6s activity on extinction retrieval. (O) Boxplots of the AUC before and after the presentation of CS during extinction retrieval ( $p = .2778$ , 2-tailed paired  $t$  test;  $n = 35$  trials/7 mice). ACC, anterior cingulate cortex; AUC, area under the curve; CS, conditioned stimuli; PPC, posterior parietal cortex.

Parietal-Frontal Pathway Controls ABC Renewal

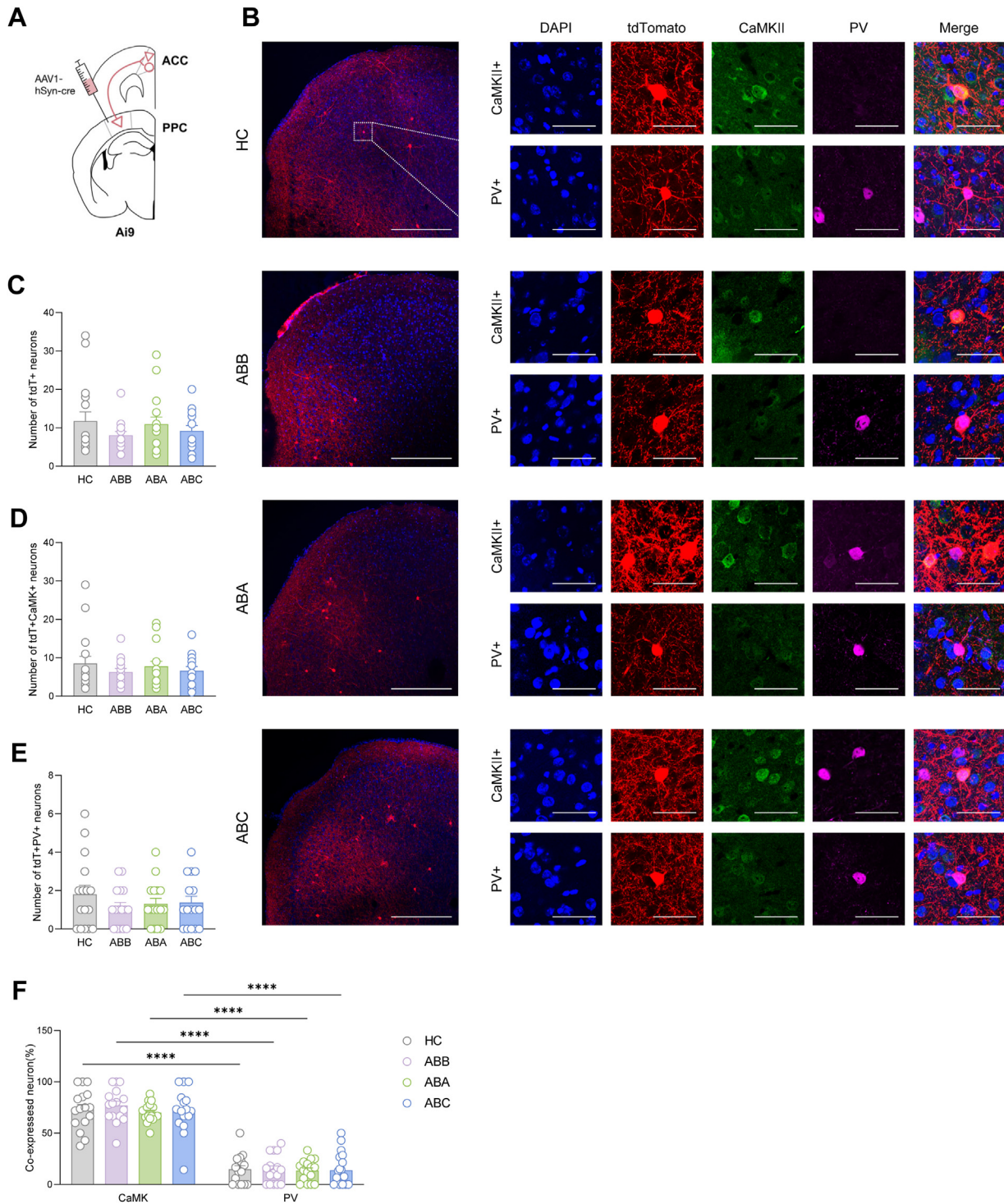


**Figure 3.** Structural characterizations of the projections from the PPC to the ACC. **(A)** Schematic experimental design for the viral injection of trans-synaptic Cre recombinase in Ai9 mice. **(B)** Representative images showing fluorescence from the trans-synaptic labeling of PPC projections (tdT+; red) costained with CaMKII<sup>+</sup> (green) and PV<sup>+</sup> (magenta) populations in the ACC. Scale bar = 500  $\mu$ m (left) or 50  $\mu$ m (right). **(C)** Quantification of tdT<sup>+</sup> neurons ( $F_{3,60} = 0.9285$ ,  $p = .4326$ , 1-way ANOVA;  $n = 16$  slices/8 mice for HC, ABB, ABA, and ABC groups, respectively). **(D)** Quantification of tdT<sup>+</sup> CaMKII<sup>+</sup> cells ( $F_{3,60} = 0.5606$ ,  $p = .6431$ , 1-way ANOVA). **(E)** Quantification of tdT<sup>+</sup> PV<sup>+</sup> cells ( $F_{3,60} = 0.7166$ ,  $p = .5459$ , 1-way ANOVA). **(F)** The ratio colocalized cells (group effect,  $F_{3,120} = 0.3393$ ,  $p = .7969$ ; cell type effect,  $F_{1,120} = 444.6$ , \*\*\*\* $p < .0001$ ; group  $\times$  cell type interaction,  $F_{3,120} = 0.3127$ ,  $p = .8162$ ; CaMKII-ABB vs. PV-ABB: \*\*\*\* $p < .0001$ ; CaMKII-ABA vs. PV-ABA: \*\*\*\* $p < .0001$ ; CaMKII-ABC vs. PV-ABC: \*\*\*\* $p < .0001$ ; 2-way ANOVA with Tukey's multiple comparisons tests). CaMKII<sup>+</sup> postsynaptic cells had more connections than PV<sup>+</sup> cells in all the groups. ACC, anterior cingulate cortex; ANOVA, analysis of variance; CaMKII, calcium/calmodulin-dependent protein kinase; HC, home cage; PPC, posterior parietal cortex; PV, parvalbumin; tdT, tdTomato.

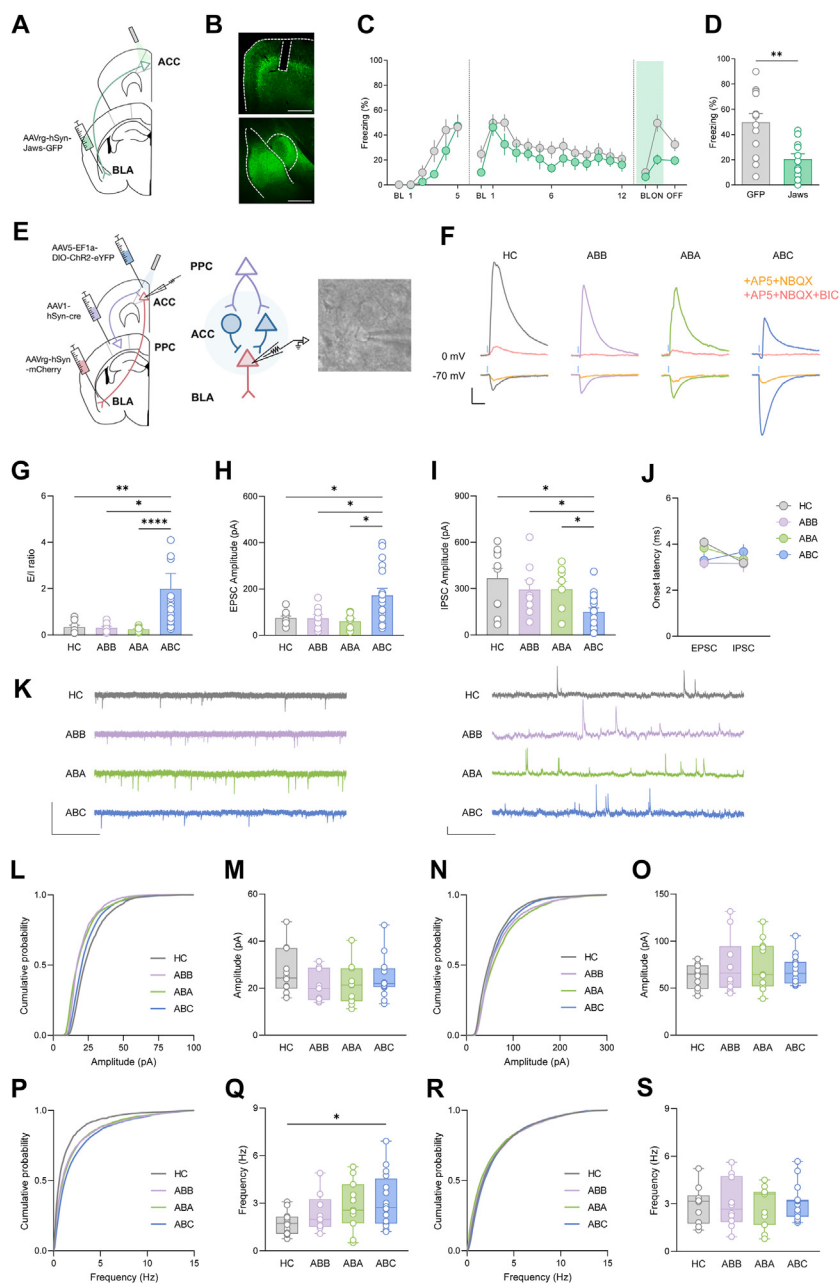


**Figure 4.** PPC-driven synaptic activity in the ACC.

**(A)** Schematic of the experimental design for the optogenetic inhibition of the ACC-to-BLA circuit. **(B)** Representative images showing the injection site of AAVrg-hSYN-Jaws-GFP in the BLA (bottom) and eYFP immunofluorescence in the ACC (top). Scale bar = 500  $\mu$ m. **(C)** ABC fear renewal with optogenetic inhibition of ACC-BLA projections (group effect:  $F_{1,22} = 2.412$ ,  $p = .1347$ ; time effect:  $F_{21,462} = 16.27$ ,  $***p < .0001$ ; group  $\times$  time interaction:  $F_{21,462} = 1.272$ ,  $p = .1884$ ; 2-way repeated-measures ANOVA). **(D)** Optogenetic activation of ACC-BLA projections significantly reduced freezing during ABC renewal ( $**p = .0026$ , 2-tailed unpaired  $t$  test;  $N = 13$  and 11 for GFP and Jaws, respectively). **(E)** Schematic of experimental design for ex vivo electrophysiology recording (left) of mCherry-expressing ACC neurons projecting to the BLA without the concurrent expression of ChR2 were recorded under optogenetic stimulation (middle), an example image of a recorded neuron in the ACC (right). **(F)** Representative example traces of ACC pyramidal neurons in response to photostimulation by BLA-projecting ACC neurons receiving projections from the PPC. **(G)** E/I ratio (HC vs. ABB:  $p = .9654$ ; HC vs. ABA:  $p = .8968$ ; HC vs. ABC:  $***p = .0004$ ; ABB vs. ABA:  $p = .6454$ ; ABB vs. ABC:  $***p = .0009$ ; ABA vs. ABC:  $****p < .0001$ ; Mann-Whitney  $U$  test,  $n = 10$  cells/5 mice, 8 cells/3 mice, 8 cells/4 mice, and 17 cells/8 mice for HC, ABB, ABA, and ABC, respectively). **(H)** Optogenetically evoked EPSC amplitudes (HC vs. ABB:  $p = .8968$ ; HC vs. ABA:  $p = .7618$ ; HC vs. ABC:  $*p = .0404$ ; ABB vs. ABA:  $p = .7209$ ; ABB vs. ABC:  $*p = .0313$ ; ABA vs. ABC:  $*p = .0190$ ; Mann-Whitney  $U$  test). **(I)** Optogenetically evoked IPSC amplitudes (HC vs. ABB:  $p = .5726$ ; HC vs. ABA:  $p = .3154$ ; HC vs. ABC:  $*p = .0151$ ; ABB vs. ABA:  $p = .7984$ ; ABB vs. ABC:  $*p = .0495$ ; ABA vs. ABC:  $*p = .0266$ ; Mann-Whitney  $U$  test). **(J)** Onset latency of evoked response (group effect,  $F_{3,78} = 0.6633$ ,  $p = .5771$ ; E-I effect,  $F_{1,78} = 1.153$ ,  $p = .2863$ ; group  $\times$  time interaction,  $F_{3,78} = 1.645$ ,  $p = .1859$ ; 2-way ANOVA). **(K)** Voltage-clamp recordings of sEPSCs (left) and spontaneous sIPSCs (right). **(L)** Cumulative distribution of sEPSC amplitude. The sEPSC amplitude and kinetics did not differ among the 4 groups (HC vs. ABB:  $p = .0166$ ; HC vs. ABA:  $p = .1585$ ; HC vs. ABC:  $p = .9093$ ; ABB vs. ABA:  $p = .8175$ ; ABB vs. ABC:  $p = .0809$ ; ABA vs. ABC:  $p = .4740$ ; KS test). **(M)** Average sEPSC amplitudes ( $F_{3,46} = 0.6491$ ,  $p = .5880$ , 1-way ANOVA;  $n = 14$  cells/6 mice, 9 cells/5 mice, 11 cells/4 mice, and 16 cells/6 mice for the HC, ABB, ABA, and ABC groups, respectively). **(N)** Cumulative distribution of sIPSC amplitudes (HC vs. ABB,  $p = .1585$ ; HC vs. ABA,  $p = .1144$ ; HC vs. ABC,  $p = .9997$ ; ABB vs. ABA,  $p = .9941$ ; ABB vs. ABC,  $p = .2864$ ; ABA vs. ABC,  $p = .2153$ ; KS test). **(O)** Average sIPSC amplitudes ( $F_{3,42} = 0.7337$ ,  $p = .5378$ , 1-way ANOVA;  $n = 10$  cells/5 mice, 10 cells/5 mice, 11 cells/4 mice, and 15 cells/6 mice for HC, ABB, ABA, and ABC groups, respectively). **(P)** Cumulative distribution of sEPSC frequency (HC vs. ABB:  $***p = .0006$ ; HC vs. ABA:  $***p = .0009$ ; HC vs. ABC:  $***p = .0001$ ; ABB vs. ABA:  $p = .9839$ ; ABB vs. ABC:  $p = .9969$ ; ABA vs. ABC:  $p = .7269$ ; KS test). **(Q)** Average sEPSC frequency ( $F_{3,46} = 3.065$ ,  $*p = .0372$ ; HC vs. ABC:  $*p = .0273$ , 1-way ANOVA with Tukey's multiple comparison test). **(R)** Cumulative distribution of sIPSC frequency (HC vs. ABB,  $p > .9999$ ; HC vs. ABA,  $p > .9999$ ; HC vs. ABC,  $p = .9998$ ; ABB vs. ABA,  $p > .9999$ ; ABB vs. ABC,  $p = .9839$ ; ABA vs. ABC,  $p = .9998$ ; KS test). **(S)** Average sIPSC frequency ( $F_{3,42} = 0.08907$ ,  $p = .9657$ , 1-way ANOVA). ACC, anterior cingulate cortex; ANOVA, analysis of variance; BL, baseline; BLA, basolateral amygdala; E/I, excitation/inhibition; eYFP, enhanced yellow fluorescent protein; GFP, green fluorescent protein; HC, home cage; KS, Kolmogorov-Smirnov; PPC, posterior parietal cortex; sEPSC, spontaneous excitatory postsynaptic current; sIPSC, spontaneous inhibitory postsynaptic current.

(NpHR+Sal – NpHR+Flx) (Figure 6D, E). In a parallel experiment, B6 mice underwent the same procedure for Chr2 expression in the PPC  $\rightarrow$  ACC pathway. The Chr2+Sal group

displayed an increase in fear response, whereas the Chr2+Flx group exhibited a decrease in the optogenetically induced fear response (Figure 6F–H).



Parietal-Frontal Pathway Controls ABC Renewal

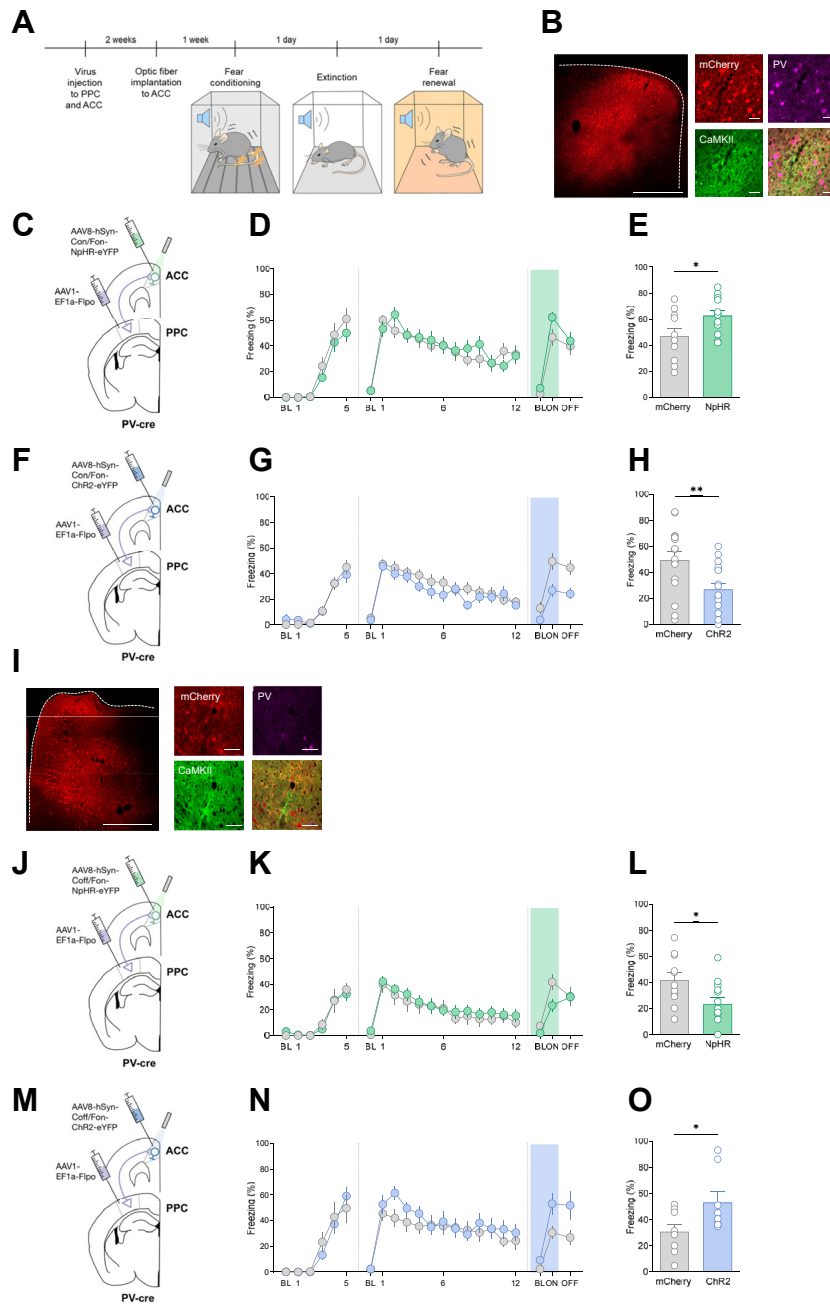


**Figure 5.** PPC→ACC<sup>PV</sup> neurons bidirectionally modulate ABC renewal. **(A)** Schematic representation of the experimental schedule for the optogenetic manipulation of subpopulations of ACC neurons that receive projections from the PPC during ABC renewal. **(B)** Representative image showing PPC→ACC<sup>PV</sup> neurons (red) costained with CaMKII+ (green) and PV+ (magenta) in the ACC. Scale bar = 500 μm (left) or 50 μm (right). **(C)** Schematic representation of viral infection and optic fiber implantation for the photoinhibition of the PPC→ACC<sup>PV</sup> circuit. **(D)** ABC renewal with optogenetic inhibition of the PPC→ACC<sup>PV</sup> circuit (group effect,  $F_{1,21} = 0.00297$ ,  $p = .8648$ ; time effect,  $F_{21,441} = 38.64$ ,  $****p < .0001$ ; group × time interaction,  $F_{21,441} = 1.297$ ,  $p = .1710$ ; 2-way RM ANOVA). **(E)** Photoinhibition of the PPC→ACC<sup>PV</sup> neurons significantly evoked the release of fear memory ( $*p = .0345$ , 2-tailed unpaired  $t$  test;  $N = 10$  and 13 for mCherry and NpHR, respectively). **(F)** Schematic of viral infection and optic fiber implantation for the photoactivation of PPC→ACC<sup>PV</sup> projections. **(G)** ABC renewal with optogenetic activation of PPC→ACC<sup>PV</sup> projections (group effect,  $F_{1,23} = 0.3999$ ,  $p = .5334$ ; time effect,  $F_{21,483} = 34.13$ ,  $****p < .0001$ ; group × time interaction,  $F_{21,483} = 0.8786$ ,  $p = .6197$ ; 2-way RM ANOVA). **(H)** The Chr2 group showed significantly reduced fear responses during ABC renewal ( $**p = .0079$ , 2-tailed unpaired  $t$  test;  $N = 16$  and 17 for mCherry and Chr2, respectively). **(I)** A representative image showing PPC→ACC non-PV neurons (red) costained with CaMKII+ (green) and PV+ (magenta) populations in the ACC. Scale bar = 500 μm (left) or 50 μm (right). **(J)** Schematic of viral infection and optic fiber implantation for photoinhibition of the non-PV population of the PPC→ACC circuit. **(K)** ABC renewal with optogenetic inhibition of the non-PV population of the PPC→ACC circuit (group effect,  $F_{1,22} = 0.02621$ ,  $p = .8729$ ; time effect,  $F_{21,462} = 18.05$ ,  $****p < .0001$ ; group × time interaction,  $F_{21,462} = 0.8128$ ,  $p = .7049$ ; 2-way RM ANOVA). **(L)** Photoinhibition of the non-PV population of the PPC→ACC circuit showed decreased the fear response ( $*p = .0220$ , 2-tailed unpaired  $t$  test;  $N = 11$  and 13 for mCherry and NpHR, respectively). **(M)** Schematic of viral infection and optic fiber implantation for activation of the non-PV population of the PPC→ACC circuit. **(N)** ABC renewal with optogenetic activation of the non-PV population of the PPC→ACC circuit (group effect,  $F_{1,15} = 0.9306$ ,  $p = .3500$ ; time effect,  $F_{21,315} = 22.41$ ,  $****p < .0001$ ; group × time interaction,  $F_{21,315} = 1.431$ ,  $p = .1014$ ; 2-way RM ANOVA). **(O)** Photoactivation of the non-PV population of the PPC→ACC circuit resulted in an increased fear response ( $*p = .0340$ , 2-tailed unpaired  $t$  test;  $N = 9$  and 8 for mCherry and NpHR, respectively).

unpaired  $t$  test;  $N = 9$  and 8 for mCherry and NpHR, respectively). ACC, anterior cingulate cortex; ANOVA, analysis of variance; BL, baseline; CaMKII, calcium/calmodulin-dependent protein kinase; PPC, posterior parietal cortex; PV, parvalbumin; RM, repeated-measures.

Furthermore, in slice physiology experiments, fluoxetine administration resulted in a decrease in evoked EPSC and IPSC, indicating that the effects of fluoxetine extended to the synaptic level (Figure 6L–L). This suggests that the effects of fluoxetine on synaptic transmission may contribute to its role in attenuating fear responses to ABC renewal.

Next, we explored the potential impact of fluoxetine on general mouse behavior to determine whether its effects are

reflective of the overall state of the mice irrespective of concurrent optogenetic manipulation. To test this, we conducted a series of behavioral assays, including the open field, Y-maze, and novel object recognition test, following the administration of fluoxetine (Figure S7A). These results indicate that fluoxetine administration did not significantly influence the general state of the mice, including anxiety, locomotor activity, working memory, and long-term memory. Instead, they suggest that

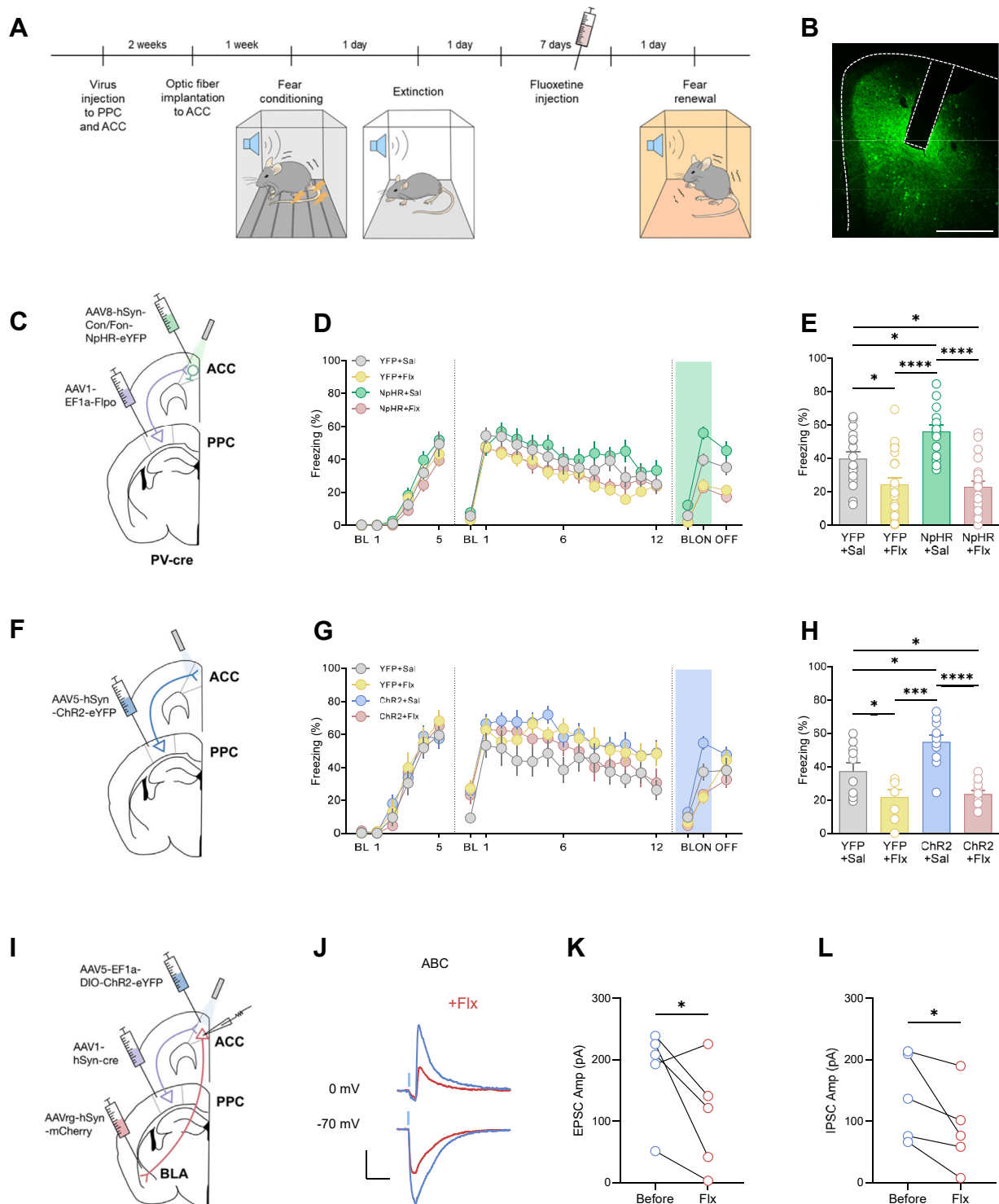


**Figure 6.** Flx treatment attenuated the optogenetically induced relapse of fear memory. **(A)** Schematic representation of the experimental schedule for ABC renewal with Flx treatment. **(B)** PPC→ACC<sup>PV</sup> neurons with the tip of an optic fiber placement. Scale bar = 500 μm. **(C)** Schematic of viral infection and optic fiber implantation for photoinhibition of PPC→ACC<sup>PV</sup> neurons. **(D)** ABC renewal with optogenetic inactivation of the PPC→ACC<sup>PV</sup> circuit after chronic administration of Flx (group effect,  $F_{1,75} = 0.7321, p = .3949$ ; drug effect,  $F_{1,75} = 9.002, **p = .0037$ ; time effect,  $F_{21,1575} = 94.26, ****p < .0001$ ; group × time interaction,  $F_{21,1575} = 1.047, p = .4011$ ; drug × time interaction,  $F_{21,1575} = 3.867, ****p < .0001$ ; group × drug interaction,  $F_{1,75} = 0.6683, p = .4162$ ; group × drug × time interaction,  $F_{21,1575} = 0.8622, p = .6419$ ; 3-way repeated-measures ANOVA). **(E)** The Flx treatment significantly blocked the optogenetically evoked

the effect of fluoxetine is linked to the specific context in which it is administered, potentially impacting specific neural circuits targeted by optogenetic manipulation rather than exerting a broad influence on overall mouse behavior.

## DISCUSSION

Fear-related disorders are clinically challenging to treat because the symptoms, which are characterized by the association of traumatic events with fear and generalization to a variety of stimuli that are not present during the traumatic event, often persist even after ongoing exposure-based therapy (3,54). Therefore, understanding fear renewal, characterized by the relapse of extinguished fear responses in novel or neutral contexts after extinction, is crucial for studying fear-related psychiatric disorders (12,13,55–57). The ABC renewal model suggests that the reappearance of fear following exposure therapy is more likely when the individual encounters the feared stimulus in a novel context compared with the original acquisition context (ABA renewal). Animal studies suggests that ABC renewal may be weaker than ABA renewal, requiring stronger contextual manipulations for detection in humans (58–63). Recent studies using robust context manipulations have provided evidence for ABC renewal (58,60,62). These findings emphasize the importance of context in fear responses, informing interventions to prevent fear relapse after exposure therapy. Patients are often exposed to neutral stimuli in novel or neutral situations, triggering fear relapse through the ABC renewal mechanism rather than in the traumatic context in which fear was originally acquired (55,58,60–62,64–66). Therefore, discriminating between ABC and ABA renewal mechanisms is essential for developing more targeted and effective treatments for fear-related psychiatric disorders, including understanding the specific neural circuits underlying each type of renewal.

Notably, the PPC→ACC circuit plays a key role in the novel context-dependent relapse of extinguished fear memory, in which target neurons in the ACC are only responsive to ABC renewal. In contrast, previous studies have focused on the importance of the relationship between the vHPC and IL in ABA renewal. Inhibition of vHPC to the central nucleus of the amygdala and vHPC→IL circuits suppresses fear renewal in a conditioning context, i.e., ABA renewal (8,38). Particularly, the activation of vHPC→IL projections promotes fear relapse in the extinction context, suggesting that vHPC→IL projections

suppress the expression of extinction, leading to a relapse of extinguished fear in the extinction context (38). Together, these studies indicate that the vHPC→IL circuit bidirectionally modulates the relapse of fear memory in a conditioning context, showing distinct characteristics of PPC→ACC neurons that are only responsive to a novel context.

Specialized cell types and mechanisms underlying ABC renewal have not yet been identified. In an earlier study, PV interneurons were found to play a regulatory role in ABA renewal by mediating vHPC-driven feed-forward inhibition of amygdala-projecting pyramidal neurons in the IL (38). Similarly, we found that PPC→ACC<sup>PV</sup> interneurons regulated novel context-dependent fear renewal. Our ex vivo experiments revealed that network synaptic activity in PPC→ACC neurons significantly increased after ABC renewal owing to the effect of enhanced excitatory currents and dampened inhibitory currents. Our approach, using circuit- and cell type-specific optogenetics, demonstrated the necessity and sufficiency of PV cells in the regulation of fear memory relapse in a novel context. However, additional studies are needed to provide direct evidence of behavioral state-dependent plasticity and PV-mediated regulatory mechanisms for ABC renewal. However, these results revealed a previously unidentified role for PV neurons in the ACC in context-dependent fear renewal.

Among the various pharmacological medications available for fear-related disorders, first-line treatments include antidepressants and anxiolytic classes, such as serotonin and other monoamine reuptake inhibitors (49,63,67). Although there is growing evidence of monoaminergic regulation of fear circuits, their specific actions remain unclear (49–52). Despite the amount of research in this area, there is little evidence of fear renewal in ABCs. In this study, chronic injections of fluoxetine successfully disrupted ABC fear renewal behavior. Although more research is required to better understand the neural mechanisms by which fluoxetine interacts with the PPC→ACC→BLA circuit for ABC renewal, this study suggests that this novel circuitry mechanism of fear renewal may enhance our understanding of context-dependent fear memory.

## ACKNOWLEDGMENTS AND DISCLOSURES

This work was supported by the National Research Foundation of Korea, South Korea grants funded by the Ministry of Education (Grant No. NRF-2020R1A6A3A1307717711 [to BJJ]), Ministry of Science and Information and Communication Technology (Grant No. NRF-2022M3E5E8081182

high level of fear response in the PV mice (group effect,  $F_{1,75} = 3.762$ ,  $p = .0562$ ; drug effect,  $F_{1,75} = 40.14$ ,  $****p < .0001$ ; group  $\times$  drug interaction,  $F_{1,75} = 5.368$ ,  $*p = .0232$ ; YFP+Sal vs YFP+Flx,  $*p = .0270$ ; YFP+Sal vs NpHR+Sal,  $*p = .0332$ ; YFP+Sal vs NpHR+Flx,  $*p = .0128$ ; YFP+Flx vs. NpHR+Sal,  $****p < .0001$ ; NpHR+Sal vs NpHR+Flx,  $****p < .0001$ , 2-way ANOVA with Tukey's multiple comparisons tests;  $N = 17, 23, 16$ , and  $23$  for YFP+Sal, YFP+Flx, NpHR+Sal, and NpHR+Flx, respectively). (F) Schematic representation of viral infection and optic fiber implantation for the photoinhibition of the PPC→ACC circuit. (G) ABC renewal with optogenetic stimulation of the PPC→ACC circuit after chronic administration of Flx (group effect,  $F_{1,37} = 0.9185$ ,  $p = .3441$ ; drug effect,  $F_{1,37} = 0.008941$ ,  $p = .9252$ ; time effect,  $F_{21,777} = 60.01$ ,  $****p < .0001$ ; group  $\times$  time interaction,  $F_{21,777} = 1.728$ ,  $p = .6185$ ; drug  $\times$  time interaction,  $F_{21,777} = 1.728$ ,  $*p = .0225$ ; group  $\times$  drug interaction,  $F_{1,37} = 4.634$ ,  $*p = .0379$ ; group  $\times$  drug  $\times$  time interaction,  $F_{21,777} = 1.113$ ,  $p = .3276$ ; 3-way repeated-measures ANOVA). (H) The Flx treatment significantly blocked the optogenetically evoked high level of fear response in the B6 mice (group effect,  $F_{1,36} = 4.812$ ,  $*p = .0348$ ; drug effect,  $F_{1,36} = 37.79$ ,  $****p < .0001$ ; group  $\times$  drug interaction,  $F_{1,36} = 3.009$ ,  $p = .0913$ ; YFP+Sal vs YFP+Flx,  $*p = .0301$ ; YFP+Sal vs ChR2+Sal,  $*p = .0391$ ; YFP+Sal vs ChR2+Flx,  $*p = .0329$ ; YFP+Flx vs. ChR2+Sal,  $****p < .0001$ ; ChR2+Sal vs ChR2+Flx,  $****p < .0001$ ; 2-way ANOVA with Tukey's multiple comparisons tests;  $N = 9, 8, 11$ , and  $12$  for YFP+Sal, YFP+Flx, ChR2+Sal, and ChR2+Flx, respectively). (I) Schematic of the experimental design for ex vivo electrophysiology recordings. (J) Representative traces of ACC pyramidal neurons in response to photostimulation and changes induced by fluoxetine treatment. (K) Optogenetically evoked EPSC amplitude (before vs. after Flx:  $*p = .0474$ , 1-tailed paired  $t$  test). (L) Optogenetically evoked IPSC amplitude (before vs. Flx:  $*p = .0319$ , 1-tailed paired  $t$  test). ACC, anterior cingulate cortex; ANOVA, analysis of variance; BL, baseline; BLA, basolateral amygdala; EPSC, excitatory postsynaptic current; Flx, fluoxetine; IPSC, inhibitory postsynaptic current; PPC, posterior parietal cortex; PV, parvalbumin; Sal, saline, YFP, yellow fluorescent protein.

[to JWK]), and the Korea Brain Research Institute Basic Research Program (Grant No. 23-BR-03-03 [to JWK]).

We thank Jungmin Lee and Wuhyun Koh for helpful discussions.

BJ and JWK conceived the study. BJ conducted the experiments, analyzed the data, performed the statistical analysis and figure generation, and wrote the LabVIEW and MATLAB scripts. SX, HP, and J-CR participated in the design of the study. J-CR wrote MATLAB script. KK developed multisite fiber photometry and wrote a LabVIEW script. JWK provided funding and supervised the project. BJ wrote the original draft, and JWK reviewed and edited the manuscript. All the authors reviewed the manuscript.

The customized codes used to process the data presented in this manuscript are available upon request.

The authors report no biomedical financial interests or potential conflicts of interest.

## ARTICLE INFORMATION

From the Emotion, Cognition and Behavior Research Group, Korea Brain Research Institute, Daegu, Republic of Korea (BJ, JWK); Department of Brain Sciences, Daegu Gyeongbuk Institute of Science and Technology, Daegu, Republic of Korea (BJ, HP, J-CR, JWK); Medical Research Center, Affiliated Cancer Hospital of Hainan Medical University, Haikou, Hainan, China (SX); Neurovascular Unit Research Group, Korea Brain Research Institute, Daegu, Republic of Korea (HP); Research Strategy Office, Korea Brain Research Institute, Daegu, Republic of Korea (KK); and Sensory & Motor Systems Neuroscience Research Group, Korea Brain Research Institute, Daegu, Republic of Korea (J-CR).

Address correspondence to Ja Wook Koo, Ph.D., at [jawook.koo@kbri.re.kr](mailto:jawook.koo@kbri.re.kr).

Received Jun 28, 2023; revised Feb 28, 2024; accepted Mar 25, 2024.

Supplementary material cited in this article is available online at <https://doi.org/10.1016/j.bpsgos.2024.100315>.

## REFERENCES

- Desmedt A, Marighetto A, Piazza PV (2015): Abnormal fear memory as a model for posttraumatic stress disorder. *Biol Psychiatry* 78:290–297.
- VanElzakker MB, Dahlgren MK, Davis FC, Dubois S, Shin LM (2014): From Pavlov to PTSD: The extinction of conditioned fear in rodents, humans, and anxiety disorders. *Neurobiol Learn Mem* 113:3–18.
- Vervliet B, Craske MG, Hermans D (2013): Fear extinction and relapse: State of the art. *Annu Rev Clin Psychol* 9:215–248.
- Ledoux JE (2000): Emotion circuits in the brain. *Annu Rev Neurosci* 23:155–184.
- Maren S, Quirk GJ (2004): Neuronal signalling of fear memory. *Nat Rev Neurosci* 5:844–852.
- Fanselow MS, Poulos AM (2005): The neuroscience of mammalian associative learning. *Annu Rev Psychol* 56:207–234.
- Tovote P, Fadok JP, Lüthi A (2015): Neuronal circuits for fear and anxiety. *Nat Rev Neurosci* 16:317–331.
- Xu C, Krabbe S, Gründemann J, Botta P, Fadok JP, Osakada F, *et al.* (2016): Distinct hippocampal pathways mediate dissociable roles of context in memory retrieval. *Cell* 167:961–972.e16.
- Maren S, Phan KL, Liberzon I (2013): The contextual brain: Implications for fear conditioning, extinction and psychopathology. *Nat Rev Neurosci* 14:417–428.
- Ramanathan KR, Jin J, Giustino TF, Payne MR, Maren S (2018): Prefrontal projections to the thalamic nucleus reuniens mediate fear extinction. *Nat Commun* 9:4527.
- Rozeske RR, Jercog D, Karalis N, Chaudun F, Khoder S, Girard D, *et al.* (2018): Prefrontal-periaqueductal gray-projecting neurons mediate context fear discrimination. *Neuron* 97:898–910.e6.
- Bouton ME (1988): Context and ambiguity in the extinction of emotional learning: Implications for exposure therapy. *Behav Res Ther* 26:137–149.
- Bouton ME, Westbrook RF, Corcoran KA, Maren S (2006): Contextual and temporal modulation of extinction: Behavioral and biological mechanisms. *Biol Psychiatry* 60:352–360.
- Oh SW, Son SJ, Morris JA, Choi JH, Lee C, Rah JC (2021): Comprehensive analysis of long-range connectivity from and to the posterior parietal cortex of the mouse. *Cereb Cortex* 31:356–378.
- Lyamzin D, Benucci A (2019): The mouse posterior parietal cortex: Anatomy and functions. *Neurosci Res* 140:14–22.
- Sestieri C, Shulman GL, Corbetta M (2017): The contribution of the human posterior parietal cortex to episodic memory. *Nat Rev Neurosci* 18:183–192.
- Harvey CD, Coen P, Tank DW (2012): Choice-specific sequences in parietal cortex during a virtual-navigation decision task. *Nature* 484:62–68.
- Hwang EJ, Dahlen JE, Mukundan M, Komiyama T (2017): History-based action selection bias in posterior parietal cortex. *Nat Commun* 8:1242.
- Zhou Y, Freedman DJ (2019): Posterior parietal cortex plays a causal role in perceptual and categorical decisions. *Science* 365:180–185.
- Driscoll LN, Pettit NL, Minderer M, Chettih SN, Harvey CD (2017): Dynamic reorganization of neuronal activity patterns in parietal cortex. *Cell* 170:986–999.e16.
- Raposo D, Kaufman MT, Churchland AK (2014): A category-free neural population supports evolving demands during decision-making. *Nat Neurosci* 17:1784–1792.
- Akrami A, Kopec CD, Diamond ME, Brody CD (2018): Posterior parietal cortex represents sensory history and mediates its effects on behaviour. *Nature* 554:368–372.
- Freedman DJ, Ibois G (2018): An integrative framework for sensory, motor, and cognitive functions of the posterior parietal cortex. *Neuron* 97:1219–1234.
- Snyder LH, Batista AP, Andersen RA (1997): Coding of intention in the posterior parietal cortex. *Nature* 386:167–170.
- Suzuki A, Kosugi S, Murayama E, Sasakawa E, Ohkawa N, Konno A, *et al.* (2022): A cortical cell ensemble in the posterior parietal cortex controls past experience-dependent memory updating. *Nat Commun* 13:41.
- Funamizu A, Kuhn B, Doya K (2016): Neural substrate of dynamic Bayesian inference in the cerebral cortex. *Nat Neurosci* 19:1682–1689.
- Morcos AS, Harvey CD (2016): History-dependent variability in population dynamics during evidence accumulation in cortex. *Nat Neurosci* 19:1672–1681.
- Erllich JC, Brunton BW, Duan CA, Hanks TD, Brody CD (2015): Distinct effects of prefrontal and parietal cortex inactivations on an accumulation of evidence task in the rat. *eLife* 4:e05457.
- Joo B, Koo JW, Lee S (2020): Posterior parietal cortex mediates fear renewal in a novel context. *Mol Brain* 13:16.
- Etkin A, Egner T, Kalisch R (2011): Emotional processing in anterior cingulate and medial prefrontal cortex. *Trends Cogn Sci* 15:85–93.
- Frankland PW, Bontempi B, Tolton LE, Kaczmarek L, Silva AJ (2004): The involvement of the anterior cingulate cortex in remote contextual fear memory. *Science* 304:881–883.
- Kim SW, Kim M, Baek J, Latchoumane CF, Gangadharan G, Yoon Y, *et al.* (2023): Hemispherically lateralized rhythmic oscillations in the cingulate-amygdala circuit drive affective empathy in mice. *Neuron* 111:418–429.e4.
- Jhang J, Lee H, Kang MS, Lee HS, Park H, Han JH (2018): Anterior cingulate cortex and its input to the basolateral amygdala control innate fear response. *Nat Commun* 9:2744.
- Allsop SA, Wichmann R, Mills F, Burgos-Robles A, Chang CJ, Felix-Ortiz AC, *et al.* (2018): Corticoamygdala transfer of socially derived information gates observational learning. *Cell* 173:1329–1342.e18.
- Maren S (2011): Seeking a spotless mind: Extinction, deconsolidation, and erasure of fear memory. *Neuron* 70:830–845.
- de Lima MAX, Baldo MVC, Oliveira FA, Canteras NS (2022): The anterior cingulate cortex and its role in controlling contextual fear memory to predatory threats. *eLife* 11:1–37.
- Einarsson EÖ., Nader K (2012): Involvement of the anterior cingulate cortex in formation, consolidation, and reconsolidation of recent and remote contextual fear memory. *Learn Mem* 19:449–452.
- Marek R, Jin J, Goode TD, Giustino TF, Wang Q, Acca GM, *et al.* (2018): Hippocampus-driven feed-forward inhibition of the prefrontal

- cortex mediates relapse of extinguished fear. *Nat Neurosci* 21:384–392.
39. Kitanishi T, Tashiro M, Kitanishi N, Mizuseki K (2022): Intersectional, anterograde transsynaptic targeting of neurons receiving mono-synaptic inputs from two upstream regions. *Commun Biol* 5:149.
  40. Zingg B, Chou XL, Zhang ZG, Mesik L, Liang F, Tao HW, Zhang LI (2017): AAV-mediated anterograde transsynaptic tagging: mapping corticocollicular input-defined neural pathways for defense behaviors. *Neuron* 93:33–47.
  41. Isosaka T, Matsuo T, Yamaguchi T, Funabiki K, Nakanishi S, Kobayakawa R, Kobayakawa K (2015): Htr2a-expressing cells in the central amygdala control the hierarchy between innate and learned fear. *Cell* 163:1153–1164.
  42. Gross CT, Canteras NS (2012): The many paths to fear. *Nat Rev Neurosci* 13:651–658.
  43. Vazdarjanova A, Cahill L, McGaugh JL (2001): Disrupting basolateral amygdala function impairs unconditioned freezing and avoidance in rats. *Eur J Neurosci* 14:709–718.
  44. Lee J, Choi JH, Rah JC (2020): Frequency-dependent gating of feedforward inhibition in thalamofrontal synapses. *Mol Brain* 13:68.
  45. Wonders CP, Anderson SA (2006): The origin and specification of cortical interneurons. *Nat Rev Neurosci* 7:687–696.
  46. Courtin J, Chaudun F, Rozeske RR, Karalis N, Gonzalez-Campo C, Wurtz H, *et al.* (2014): Prefrontal parvalbumin interneurons shape neuronal activity to drive fear expression. *Nature* 505:92–96.
  47. Hafner G, Witte M, Guy J, Subhashini N, Fenno LE, Ramakrishnan C, *et al.* (2019): Mapping brain-wide afferent inputs of parvalbumin-expressing GABAergic neurons in barrel cortex reveals local and long-range circuit motifs. *Cell Rep* 28:3450–3461.e8.
  48. Fenno LE, Ramakrishnan C, Kim YS, Evans KE, Lo M, Vesuna S, *et al.* (2020): Comprehensive dual- and triple-feature intersectional single-vector delivery of diverse functional payloads to cells of behaving mammals. *Neuron* 107:836–853.e11.
  49. Oh SJ, Cheng J, Jang JH, Arace J, Jeong M, Shin CH, *et al.* (2020): Hippocampal mossy cell involvement in behavioral and neurogenic responses to chronic antidepressant treatment. *Mol Psychiatry* 25:1215–1228.
  50. Karpova NN, Pickenhagen A, Lindholm J, Tiraboschi E, Kulesskaya N, Ágústsdóttir A, *et al.* (2011): Fear erasure in mice requires synergy between antidepressant drugs and extinction training. *Science* 334:1731–1734.
  51. Popova D, Ágústsdóttir A, Lindholm J, Mazulis U, Akamine Y, Castrén E, Karpova NN (2014): Combination of fluoxetine and extinction treatments forms a unique synaptic protein profile that correlates with long-term fear reduction in adult mice. *Eur Neuropharmacol* 24:1162–1174.
  52. Gunduz-Cinar O, Flynn S, Brockway E, Kaugars K, Baldi R, Ramikie TS, *et al.* (2016): Fluoxetine facilitates fear extinction through amygdala endocannabinoids. *Neuropsychopharmacology* 41:1598–1609.
  53. Wang Y, Yin XY, He X, Zhou CM, Shen JC, Tong JH (2021): Parvalbumin interneuron-mediated neural disruption in an animal model of postintensive care syndrome: Prevention by fluoxetine. *Aging* 13:8720–8736.
  54. Hermans D, Craske MG, Mineka S, Lovibond PF (2006): Extinction in human fear conditioning. *Biol Psychiatry* 60:361–368.
  55. Shi YW, Fan BF, Xue L, Wang XG, Ou XL (2019): Fear renewal activates cyclic adenosine monophosphate signaling in the dentate gyrus. *Brain Behav* 9:e01280.
  56. Bouton ME, García-Gutiérrez A, Zilski J, Moody EW (2006): Extinction in multiple contexts does not necessarily make extinction less vulnerable to relapse. *Behav Res Ther* 44:983–994.
  57. Bouton ME, Maren S, McNally GP (2021): Behavioral and neurobiological mechanisms of Pavlovian and instrumental extinction learning. *Physiol Rev* 101:611–681.
  58. Balooch SB, Neumann DL, Boschen MJ (2012): Extinction treatment in multiple contexts attenuates ABC renewal in humans. *Behav Res Ther* 50:604–609.
  59. Krisch KA, Bandarian-Balooch S, Neumann DL (2018): Effects of extended extinction and multiple extinction contexts on ABA renewal. *Learn Motiv* 63:1–10.
  60. Neumann DL, Kitlertsirivatana E (2010): Exposure to a novel context after extinction causes a renewal of extinguished conditioned responses: Implications for the treatment of fear. *Behav Res Ther* 48:565–570.
  61. Bouton ME, Todd TP (2014): A fundamental role for context in instrumental learning and extinction. *Behav Processes* 104:13–19.
  62. Bernal-Gamboa R, Juárez Y, González-Martín G, Carranza R, Sánchez-Carrasco L, Nieto J (2012): ABA, AAB and ABC renewal in taste aversion learning. *Psicológica* 33:1–13.
  63. Deslauriers J, Toth M, Der-Avakian A, Risbrough VB (2018): Current status of animal models of posttraumatic stress disorder: Behavioral and biological phenotypes, and future challenges in improving translation. *Biol Psychiatry* 83:895–907.
  64. Úngör M, Lachnit H (2008): Dissociations among ABA, ABC, and AAB recovery effects. *Learn Motiv* 39:181–195.
  65. Liddon CJ, Kelley ME, Rey CN, Liggett AP, Ribeiro A (2018): A translational analysis of ABA and ABC renewal of operant behavior. *J Appl Behav Anal* 51:819–830.
  66. Bouton ME, Todd TP, Vurbic D, Winterbauer NE (2011): Renewal after the extinction of free operant behavior. *Learn Behav* 39:57–67.
  67. Parsons RG, Ressler KJ (2013): Implications of memory modulation for post-traumatic stress and fear disorders. *Nat Neurosci* 16:146–153.